RESEARCH ARTICLE

M2 macrophages promote subconjunctival fibrosis through YAP/TAZ signalling

Yiwei Wang* (iD), Xingchen Geng*, Zhihua Guo, Dandan Chu, Ruixing Liu, Boyuan Cheng, Haohao Cui, Chengcheng Li, Jingguo Li (iD) and Zhanrong Li

Henan Eye Hospital, Henan Provincial People's Hospital, People's Hospital of Zhengzhou University, Zhengzhou, China

ABSTRACT

Purpose: To evaluate the role of M2 macrophages in subconjunctival fibrosis after silicone implantation (SI) and investigate the underlying mechanisms.

Materials and methods: A model of subconjunctival fibrosis was established by SI surgery in rabbit eyes. M2 distribution and collagen deposition were evaluated by histopathology. The effects of M2 cells on the migration (using wound-scratch assay) and activation (by immunofluorescence and western blotting) of human Tenon's fibroblasts (HTFs) were investigated.

Results: There were more M2 macrophages (CD68+/CD206+ cells) occurring in tissue samples around silicone implant at 2 weeks postoperatively. Dense collagen deposition was observed at 8 weeks after SI. *In vitro* experiment showed M2 expressed high level of CD206 and transforming growth factor-β1 (TGF-β1). The M2-conditioned medium promoted HTFs migration and the synthesis of collagen I and fibronectin. Meanwhile, M2-conditioned medium increased the protein levels of TGF-β1, TGF-βR II, p-Smad2/3, yes-associated protein (YAP), and transcriptional coactivator with PDZ-binding motif (TAZ). Verteporfin, a YAP inhibitor, suppressedTGF-β1/Smad2/3-YAP/TAZ pathway and attenuated M2-induced extracellular matrix deposition by HTFs.

Conclusions: TGF-β1/Smad2/3-YAP/TAZ signalling may be involved in M2-induced fibrotic activities in HTFs. M2 plays a key role in promoting subconjunctival fibrosis and can serve as an attractive target for anti-fibrotic therapeutics.

Introduction

Fibrosis is an important process that results from an overly driven wound-healing response and is characterized by the excessive production of extracellular matrix (ECM) components by myofibroblasts. Macrophages have been recognized as key regulators of wound healing and fibrosis [1–3]. Subconjunctival fibrosis is critical to the outcomes of several ophthalmic conditions or procedures such as glaucoma filtering surgery and pterygium. Therefore, it is important to explore and better understand the cellular mechanisms of macrophages in subconjunctival fibrosis.

Macrophages are highly plastic and exhibit functional and phenotypic versatility after tissue injury or disease. Broadly, these cells can be divided into classically activated (M1) or alternatively activated macrophages (M2) according to their activation state and functions [4]. M1 macrophages are a prototypic proinflammatory macrophage subset [4]. In contrast, M2 macrophages are polarized by Th2 cytokines IL4 and IL13 and other factors, characterized by the production of high levels of anti-inflammatory cytokines and profibrogenic factors [4, 5]. M2 macrophages are a major source of transforming growth factor β1 (TGF-β1), which is widely recognized as a key cytokine associated with fibrogenesis [3, 4, 6]. It has been reported that M2 macrophages play roles in fibrotic processes, such as pulmonary fibrosis [7–10], renal fibrosis [11, 12], dermal wound healing [13, 14], ischaemic cardiac fibrosis [15, 16] and neovascularization

[17–19]. The fibrous encapsulation (Figure 1 in Supplementary Material) is one major cause of failed glaucoma drainage surgery. CD68+ or CD206+ cells had been observed in perivalvular tissues from patients with failed Ahmed glaucoma valve (AGV) implantation surgery (Figure 2 in Supplementary Material). Thus, we speculated that M2 macrophages may be involved in subconjunctival fibrosis. Although the important role of macrophages in multiple tissue fibrosis has been recognized by researchers [3, 5, 12, 20], few studies have focused on the role of M2 macrophages in subconjunctival scar formation; the specific molecular mechanism underlying M2 cells' contribution to subconjunctival fibrosis remains poorly understood.

Recent studies have shown that the Hippo signalling pathway, which is highly evolutionarily conserved in mammals, is linked to the pathophysiology of fibrosis [21]. Yes-associated protein (YAP) and transcriptional coactivator with PDZ-binding motif (TAZ) are the key downstream transcriptional regulators of Hippo signalling. YAP/TAZ phosphorylation results in loss of transcriptional coactivator function. In contrast, unphosphorylated YAP/TAZ localizes to the nucleus and exerts its biological functions by binding to cognate transcription factors, which are predominantly members of the TEF1 family, and modulating transcription [22]. YAP/TAZ is differentially activated in distinct cell types, and their capacities are incompletely understood. Recent studies have shown that YAP/TAZ signalling exhibits extensive crosstalk with TGF-β1/Smad [23–26]. M2 macrophages are the main source of TGF-β1. The profibrotic response of fibroblasts to TGF-β1 is highly mechanosensitive. Therefore, we propose that TGF-β1/Smad2/3-YAP/TAZ signalling may be involved in the M2-induced fibrotic processes in subconjunctival fibrosis.

In the present study, we developed a rabbit model that mimics the process of subconjunctival fibrosis to evaluate the role of M2 macrophages in the early recovery phase. We further investigated the underlying mechanisms of YAP/TAZ signalling in M2-activated fibrotic behaviours of human Tenon's fibroblasts (HTFs).

Material and methods

Animals and subconjunctival fibrosis model

New Zealand White rabbits weighing 2.5–3.0 kg ($n = 9$, obtained from Huaxing Experimental Animal Farm, Zhengzhou, China) were used in this study. All animals were treated in accordance with the principles of the Declaration of Helsinki and ARRIVE guidelines. The experimental protocol was approved by the Ethics Committee of the Experimental Animal Care of Henan Eye Institute (permit number: HNEECA-2022-21). All rabbits were acclimated for 1 week before the experiment. Their eyes were examined under the slit lamp before the surgical procedures and were found to be unremarkable.

One piece of 4 mm × 3 mm sterile silicone (obtained from the silicone plate body of AGV-FP7, New World Medical, CA, USA) was used as the implant. Three rabbits did not receive any treatment and were used as controls. There were six rabbits in the silicone implantation (SI) group; the right eyes in this group underwent SI surgery as follows. After the administration of anaesthesia, the study eye was prepped with povidone-iodine. An eyelid speculum was then placed to expose the surgical field. A fornix-based peritomy was performed extending approximately 5 mm in the superotemporal quadrant, and posterior dissection was performed to separate Tenon's capsule from the globe. The silicone implant was positioned and secured 4 mm from the limbus, and a tight conjunctival closure was performed. The animals were treated with gatifloxacin eye gel (0.3%, 5 g, Xingqi, China) three times per day for 7 days to prevent infection. Slit-lamp examinations were performed to observe postoperative changes in the eyes.

Histological examinations

Three eyes with SI surgery were enucleated for double staining to identify M2 cells at 2 weeks postoperatively, and three eyes with SI surgery for analysis of collagen expression at 8 weeks postoperatively. Eyeballs from the control group served as controls. The eyeballs were excised, fixed, trimmed, dehydrated and embedded in paraffin. Thereafter, the tissue specimens were cut into 5-μm-thick sections for haematoxylin and eosin (H&E) staining. The sections were also stained using Masson's trichrome kit (G1006, Servicebio, China) to identify collagen according to the manufacturer's instructions. Immunohistochemical staining was performed to detect the expression of CD68 and CD206, as previously described [27]. In brief, the sections were deparaffinized and rehydrated. After antigen retrieval and serum blocking, the sections were subjected to immunohistochemical assays using anti-CD68 (1:200, ab955, Abcam, Cambridge, MA, USA) or anti-CD206 (1:100, DF4149, Affinity Biosciences, Cincinnati, OH, USA) primary antibodies. The slides were washed three times with phosphate-buffered saline (PBS) and incubated with the appropriate horseradish peroxidase-conjugated secondary antibody. Collagen expression was detected

by immunofluorescence staining. Briefly, sections were deparaffinized and rehydrated. After antigen retrieval, anti-collagen I antibodies (1:100, NB600-408, Novus Biologicals, Littleton, CO, USA) were added and incubated for 1 h. Then, the specimens were washed thoroughly with PBS and incubated with cyanine 3-labelled secondary antibodies at room temperature for 1 h, followed by 4'-6-diamidino-2-phenylindole (DAPI) staining. Double immunofluorescence staining of macrophages was performed using a mixture of mouse anti-CD68 (1:100, ab955, Abcam, Cambridge, MA) and rabbit anti-CD206 (1:100, DF4149, Affinity Biosciences, Cincinnati, OH, USA) primary antibodies. Immunoreactivity was evaluated using fluorescein isothiocyanate-labelled and cyanine 3-labelled secondary antibodies. Cell nuclei were counterstained with DAPI. Stained sections were imaged using a 3D digital slice scanner (3D HISTECH, Pannoramic 250Flash II, Hungary). Fiji (http://fiji.sc/) was used to perform the analysis, including area measurement and semiquantitative analysis of the median fluorescence intensity (MFI). Grouping information in both *in vivo* and *in vitro* experiments were withheld from the person who did data analysis.

M2 polarization and phenotyping

Human monocytic THP-1 cells were obtained from the Cell Bank of the Type Culture Collection of the Chinese Academy of Sciences (Shanghai, China). THP-1 cells were cultured in Roswell Park Memorial Institute (RPMI) 1640 medium (Solarbio Life Sciences, China) supplemented with 10% (v/v) fetal bovine serum (FBS) (Gibco, Gaithersburg, MD, USA) at 37 °C in a 5% CO_2 atmosphere. M0 differentiation was induced by exposure to 100 nM phorbol-12-myristate-13-acetate (PMA, P6741, Solarbio) for 48 h, followed by two washes with the culture media. M0 macrophages were polarized to the M2 phenotype by incubation with 20 ng/mL IL4 (200-04, PeproTech, Rocky Hill, NJ, USA) and IL13 (200-13, PeproTech) for 48 h. The macrophage supernatant was collected for further experiments. Adherent cells were prepared for phenotypic analysis using flow cytometry and immunofluorescence staining.

Flow cytometry

The adherent M0 and M2 macrophages were rinsed with cold PBS and detached by incubation with ETDA. For flow cytometry, the cell suspension was centrifuged and resuspended at 8×10^5 cells per sample. The cells were then stained with an allophycocyanin-conjugated monoclonal antibody against human CD206 (17-2069-42, eBioscience, San Diego, CA, USA) for 1 h to characterize the M2 phenotype. Upon labelling, the cells were washed, suspended in sheath fluid and analysed using a BD FACSCanto™ flow cytometer (BD Biosciences, USA).

Immunofluorescence

THP-1 cells were seeded at 5×10^5 cells/well into coverslip-bottomed six-well plates and stimulated with PMA alone or PMA with IL4/IL13 (as mentioned above). After fixation, permeabilization and blocking with 5% BSA, the cells were incubated with primary antibodies (anti-CD206, 1:200, sc-58986, Santa Cruz Biotechnology, CA; anti-pSTAT6, 1:200, PA5-104892, Invitrogen, Waltham, MA; anti-TGFβ1, 1:200, AF1027, Affinity, Cincinnati, OH, USA) overnight at 4 °C. After washing with PBS, secondary antibody was added. The cells were then counterstained with DAPI. The samples were examined under a Nikon fluorescence microscope. MFI was quantified using Fiji software.

Cytokine quantification by enzyme-linked immunosorbent assay

THP-1 cells were seeded at a density of 2×10^5 cells/mL in 12-well plates at a density of 1.5 mL per well. M0 and M2 stimulations were performed as previously described. The supernatant was harvested and centrifuged at 12,000 *g* for 5 min at 4 °C. Human TGF-β1 enzyme-linked immunosorbent assay (ELISA) kits (E-EL-0162c, Elabscience, China) were used to measure the level of TGF-β1 in M0 or M2 supernatants according to the manufacturer's instructions.

Primary culture of HTFs

Human Tenon's capsule samples were isolated from patients with primary open-angle glaucoma during glaucoma filtration surgery (trabeculectomy or AGV implantation) under sterile conditions. All procedures involving human tissues were performed according to the tenets of the Declaration of Helsinki and were approved by the institutional ethics review board of Henan Eye Hospital. Written informed consent was obtained from all the patients.

Primary cultures of HTFs were established as previously described [28, 29]. Briefly, Tenon's capsule samples were cut into small pieces and cultured in Dulbecco's modified Eagle's medium/nutrient mixture

F-12 (DMEM/F12, Solarbio) containing 10% FBS (Gibco, Gaithersburg, MD) and 1% penicillin/streptomycin. Human Tenon explants were maintained in 5% CO_2 at 37 °C in a humidified atmosphere, and primary HTFs were harvested as expansion cultures. Cells from passages 2 to 5 were used in subsequent experiments. HTFs were characterized by their adherent morphology and vimentin expression. Immunofluorescence staining was performed to identify the HTFs. Cells were labelled with a primary antibody against vimentin (1:500; ab45939, Abcam, Cambridge, MA, USA) and then with a secondary antibody. Cell nuclei were counterstained with DAPI.

Wound healing assay

The M2 supernatant was centrifuged and filtered through a 0.22 μm filter, after which it was mixed with DMEM/F12 culture medium at a ratio of 1:1 and used as M2 conditioned medium. A culture medium containing 2% FBS served as the control. HTFs were seeded in six-well plates at a density of 5×10^5 cells per well. When the cells reached 90% confluence, the culture medium was replaced with an FBS-free medium overnight to synchronize cell growth. Scratch wounds were then gently made in the centre of the cell monolayer using a sterile 200 μL pipette tip. The scratched wells were washed to remove cell debris and incubated with M2 conditioned medium or control medium. The gaps in each well were photographed using an inverted microscope (Olympus) at 0 and 22 h. The cellular migration area in each image was measured using the Fiji software. The data were quantified based on the area of the wounds at 0 h, which was considered 100%.

HTFs co-cultured with M2 supernatant

HTFs were seeded in cover-glass-bottomed six-well plates at a concentration of 2×10^5 cells per well. Verteporfin (S1786, Selleck Chemicals, Houston, TX) was prepared as a 1.5 mM stock in DMSO. HTFs were cultured in the presence of M2 supernatant with or without pretreatment with verteporfin for 3 h in the dark at a final concentration of 1.5 μM or in complete culture medium alone for 24 h. Immunofluorescence staining was performed to study the changes in α-smooth muscle actin (α-SMA) (1:200, 19245, CST, Danvers, MA), fibronectin (1:200, bs-13455R, Bioss, China) and collagen I (1:200, NB600-408, Novus Biologicals, Littleton, CO) expression in vitro as previously described.

Western blotting

HTFs were pretreated with either verteporfin (final concentrations 1.5 μM) or control (complete culture medium) for 3 h and sequentially incubated with M2-conditioned medium for 36 h. Cells were collected for western blot analysis as described in our previous study [27]. The total protein was extracted and quantified using a bicinchoninic acid protein assay kit (Solarbio), according to the manufacturer's instructions. Equal amounts of each protein sample were loaded onto sodium dodecyl sulphate-polyacrylamide gel electrophoresis and transferred to polyvinylidene fluoride membranes. Membranes were blocked with 5% non-fat milk for 2 h and incubated with primary antibodies specific for the target proteins overnight at 4 °C. The membranes were then washed with tris-buffered saline with Tween 20 and incubated with horseradish peroxidase-conjugated secondary antibodies on a shaker for 1 h. After washing with tris-buffered saline with Tween 20, the membranes were detected using a chemiluminescence detection system (Bio-Rad Laboratories) and analysed using the Fiji software. The following primary antibodies were used in the current study: anti-collagen I (1:500, AF7001, Affinity), anti-fibronectin (1:500, bs-13455R, Bioss), anti-TGF-β1 (1:500, AF1027, Affinity), anti-TGFβR II (1:1000, ab186838, Abcam), anti-Smad2/3 (1:500, AF6367, Affinity), anti-phospho-Smad2/3 (1:500, AF3367, Affinity), anti-YAP1 (1:500, bs-3605R, Bioss), anti-TAZ (1:500, bs-12367R, Bioss) and anti-TEF1 (1:500, PA5-37075, Invitrogen). GAPDH (1:2000, 10494-1-AP, Proteintech, Chicago, IL, USA) and β-tubulin (1:2000, 10094-1-AP, Proteintech) were used as loading controls.

Statistical analysis

All experiments were repeated at least three times. The results are reported as the means ± SD. All statistical analyses were performed using SPSS (SPSS 20.0, Inc., Armonk, NY, USA). The statistical significance of the differences between the groups was determined using Student's t-test or one-way analysis of variance. $P < 0.05$ was considered significant.

Results

Rabbit model of subconjunctival fibrosis

We performed SI surgery to mimic the process of perivalvular fibrosis. There were no instances of infection,
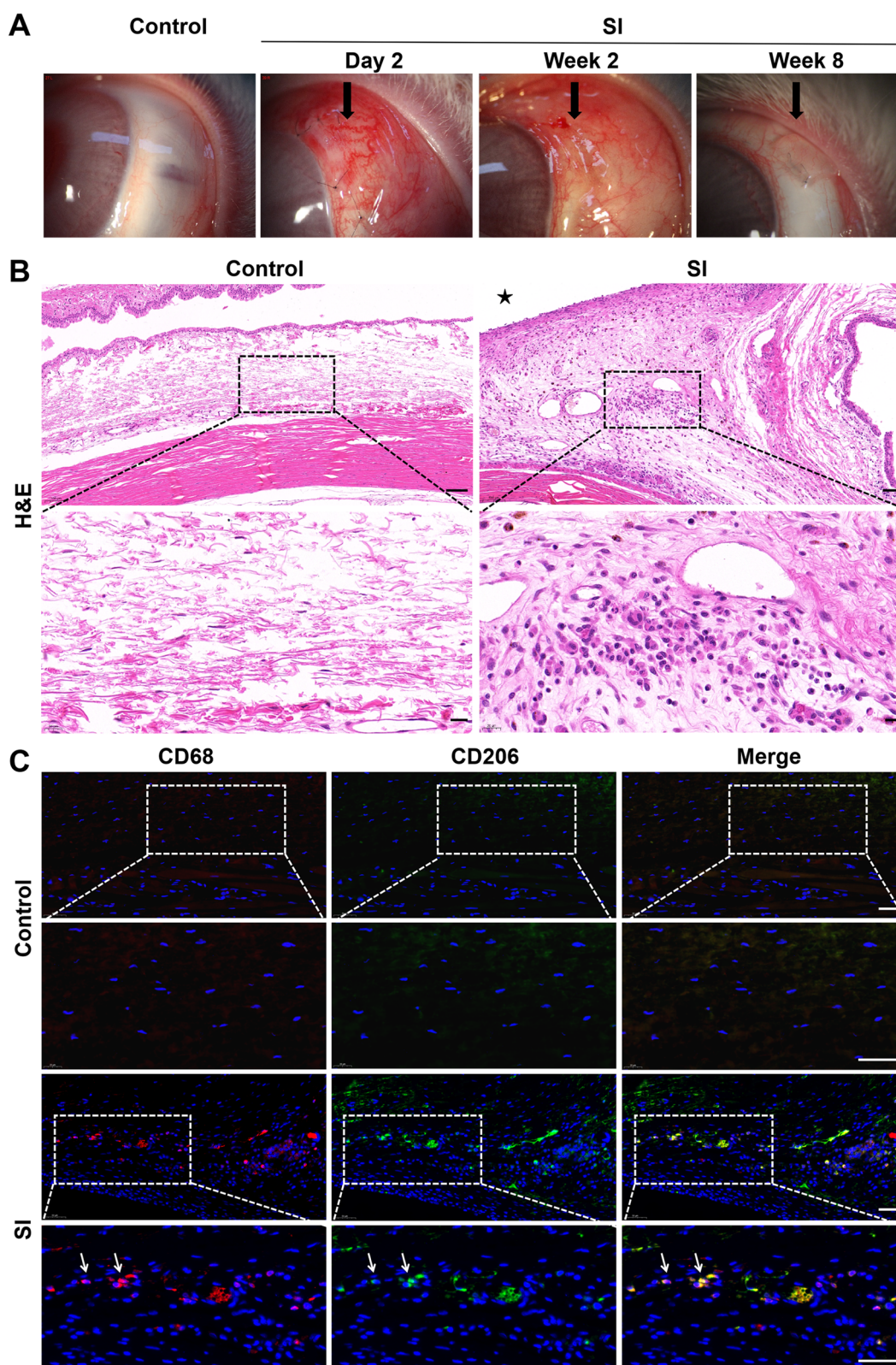
Figure 1. Histopathological evaluation in the early recovery phase following SI. Eyes with SI surgery were enucleated 2 weeks after surgery (SI group), and eyes without any treatment served as controls (*n*=3 per group). (A) Macroscopic appearance of rabbit eyes with SI showed conjunctival hyperaemia and chemosis in the early postoperative phase and thickening and fibrotic tissue in the surgical area in the late phase. Original magnification: 10×. (B) Representative micrographs of tissue sections from the controls and SI group. Black asterisk marked the position of the silicone implant. H&E staining revealed significant inflammatory cell infiltration in the surgical area. *Scale bar*: 100 μm (20 μm within the enlarged box). (C) Immunofluorescent double staining of macrophages with anti-CD68 (red) and anti-CD206 (green) antibodies. There were more CD68+/CD206+ macrophages (white arrows) in surgical areas in SI group than in the controls. *Scale bars*: 50 μm.

unexpected animal death or other complications. The macroscopic appearance of the surgical site is shown in Figure 1A. Conjunctival hyperaemia in the surgical eyes peaked in the first 1–2 days after surgery and lasted approximately 2 weeks. Mild chemosis developed and declined during the first week. Flares were not detected in the anterior chamber. Thickening and fibrotic tissue surrounding the silicone implant were observed in the surgical eyes in the late postoperative period, while a thin and translucent conjunctiva was observed in the control eyes.

Macrophages are critical regulators of tissue repair and the development of fibrosis. Two weeks after SI surgery, there was an increase in the population of inflammatory cells at the surgical site (Figure 1B). To identify the presence of M2 macrophages, we performed double immunofluorescence staining using anti-CD68 and anti-CD206 antibodies. Few macrophages were observed in the control group. By contrast, numerous CD68+ and CD206+ cells were observed in the surgical area (Figure 1C and Figure 3 in Supplementary Material).

For further analysis of subconjunctival fibrosis, rabbits were sacrificed 8 weeks after surgery, which is supposed as the late remodelling period. The tissue around the silicone implant was assessed using H&E, Masson trichrome and immunofluorescence staining. As shown in Figure 2A, H&E staining demonstrated an increase in fibroblasts and a more compact collagen deposition in the surgical area at week 8 postoperatively. Masson's trichrome staining also showed more dense collagen bundles in eyes with SI surgery compared with the controls (P < 0.001; Figure 2B,C). Fluorescent immunohistochemistry revealed a
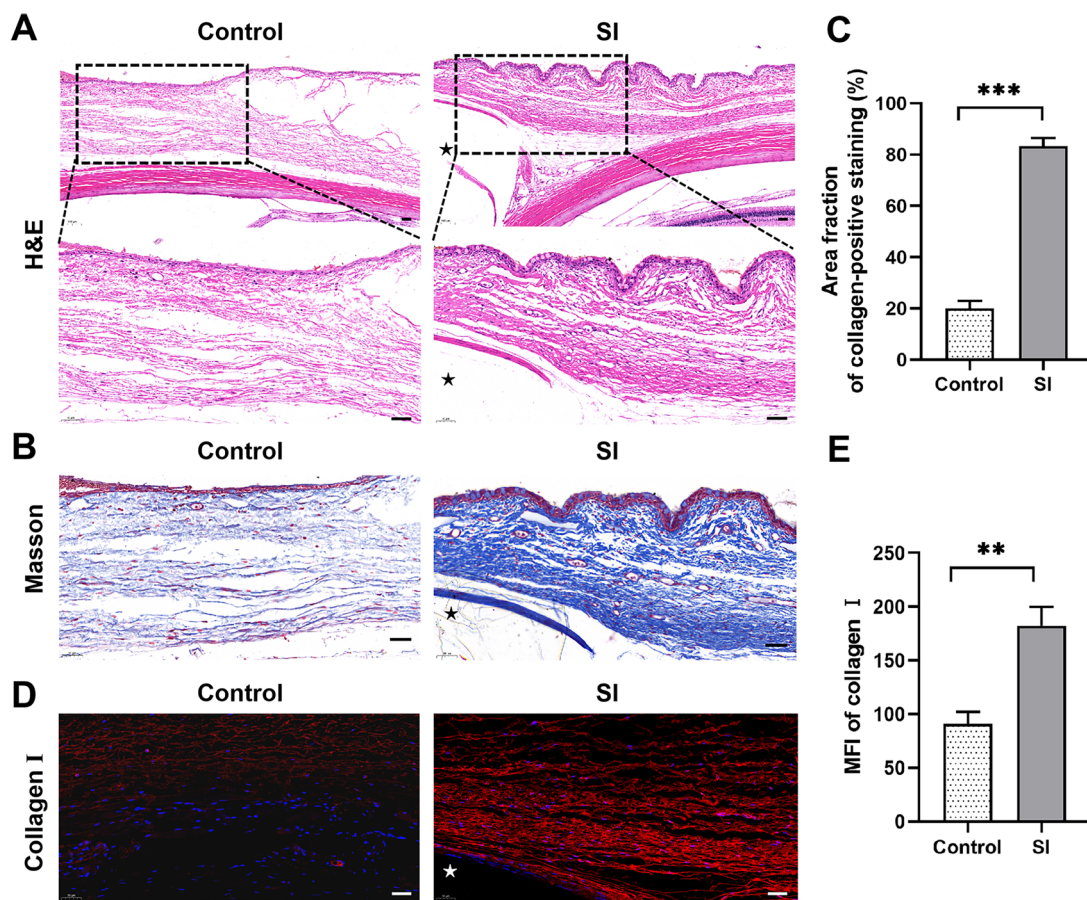
Figure 2. Histopathological assessment in the late remodelling phase following SI. Three eyes with SI surgery were enucleated 8 weeks after surgery (the SI group), and rabbits without any treatment served as controls (n = 3 per group). (A) H&E staining showed a more fusiform fibroblast-like appearance of cells (black arrows) and more compact collagen deposition surrounding the implant compared to the controls. Black asterisk marked the position of the silicone implant. *Scale bar*: 100 μm (50 μm within the enlarged box). (B) Masson's trichrome staining demonstrated dense collagen bundles in blue. Black asterisk marked the position of the silicone implant. (C) Quantification of the Masson's trichrome staining results. *Scale bars*: 50 μm. ***P < 0.001 compared to the controls; n = 3. (D) Immunofluorescence revealed significant expression of collagen I (red staining). White asterisk marked the position of the silicone implant. (E) Quantification of immunofluorescence staining for collagen I. *Scale bars*: 50 μm. **P < 0.01 compared to the controls; n = 3.
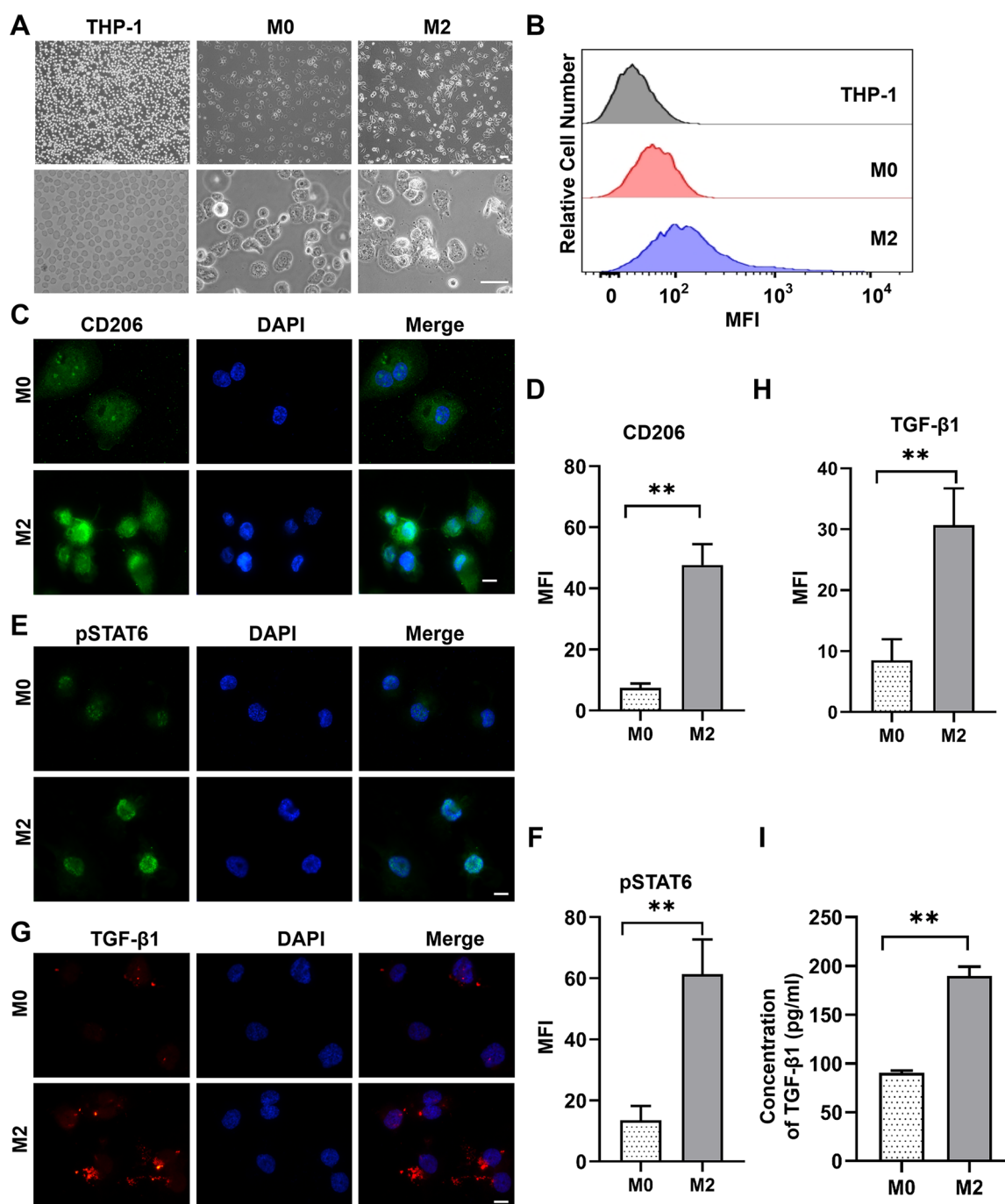
Figure 3. Differentiation of THP-1 cells into alternatively activated (M2) macrophages. (A) Different morphologic appearances of THP-1 cells that were untreated (THP-1), treated with PMA (M0) or treated with PMA and subsequently with IL4/IL13 (M2). THP-1 cells grew in suspension, while M0 and M2 were larger with increased adherence and more granules in the cytoplasm. *Scale bar*: 50 μm. (B) Representative flow cytometric analysis of untreated THP-1, M0 and M2 cells stained with allophycocyanin-conjugated monoclonal antibody anti-CD206. The MFI is shown on the *x*-axis, and the relative cell number on the *y*-axis. (C) Representative immunofluorescence images showing increased expression of CD206 in M2 cells compared to M0 macrophages. *Scale bars*: 10 μm. (D) Quantification of the results in (C). **$P < 0.01$; $n = 3$. (E) Representative immunofluorescence images showing stronger staining of pSTAT6 in M2 cells than that in M0 macrophages. *Scale bars*: 10 μm. (F) Quantification of the results in (E). **$P < 0.01$; $n = 3$. (G) Representative immunofluorescence images showing that the expression of TGF-β1 in M2 macrophages was stronger than in M0 macrophages. *Scale bar*: 10 μm. (H) Quantification of the results in (G). **$P < 0.01$; $n = 3$. (I) ELISA analysis of the cytokine TGF-β1 in M2 supernatant. **$P < 0.01$; $n = 3$. Similar results were obtained in three independent experiments.

significant expression of collagen I ($P < 0.01$; Figure 2D,E). These data confirmed increased collagen deposition following SI surgery compared to that in the controls.

Identification of M2 macrophages in vitro

Figure 3A shows the morphological characteristics of the M2 macrophages derived from THP-1 cells. THP-1 cells were small, oval cells, while PMA-differentiated THP-1 macrophages (M0) were larger, with increased adherence and more granules in the cytoplasm. After incubation with 20 ng/mL IL4 and IL13 for 48 h, M0 macrophages were polarized into M2 cells with enhanced granularity. Figure 3B shows significantly higher expression of CD206 (one marker of M2) in M2 macrophages than in M0 macrophages by flow cytometry. Immunofluorescence labelling showed higher protein levels of CD206 ($P < 0.01$; Figure 3C,D) and phospho-STAT6 (a major transcription factor responsible for M2 polarization; $P < 0.01$; Figure 3E,F) in M2 cells compared to that in M0 macrophages. Immunofluorescence staining showed that the expression level of TGF-β1 in M2 macrophages was higher than that in M0 macrophages ($P < 0.01$; Figure 3G,H). ELISA showed that the concentration of TGF-β1 was higher following treatment with PMA plus IL4/IL13 than following treatment with PMA alone ($P < 0.01$; Figure 3I). These data indicated that THP-1 cells were successfully activated and polarized into M2 macrophages.
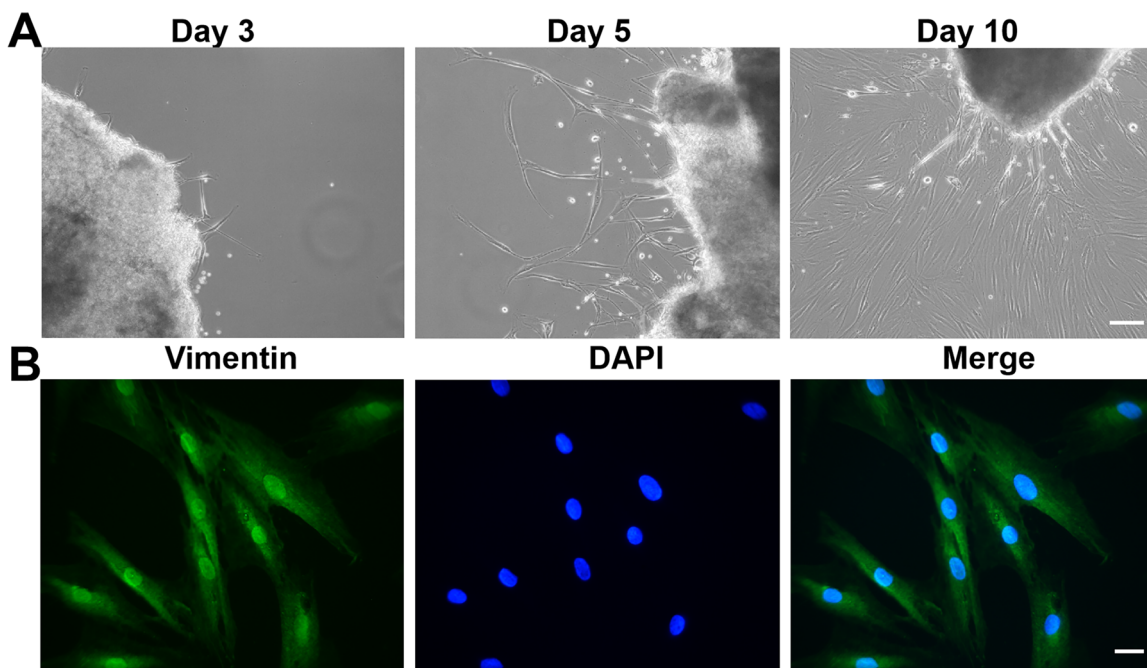
Primary HTF culture and characterization

A small number of cells migrated out of the tissue explants of human Tenon's capsule within 3–5 days of primary culture. The cells adhered to the bottom of the culture dish and exhibited a spindly and elongated phenotype. After 10 days, the cells reached sub-confluence (80%; Figure 4A). HTFs cultured in monolayers were identified as fibroblasts by intense immunostaining for vimentin (Figure 4B).

Effect of M2 macrophages on the migration of HTFs

The scratch wound healing assay was used to evaluate the influence of M2 macrophages on the migration of HTFs. As shown in Figure 5A,B, the M2-conditioned medium significantly enhanced the migratory capacity of HTFs compared to the blank control ($P < 0.01$).

Effect of M2 macrophages on HTF activation and ECM synthesis

To evaluate the effect of M2 macrophages on HTF activation and ECM synthesis, we used immunofluorescence staining to examine the expression of α-SMA, fibronectin and collagen I in HTFs cultured with blank control or M2-conditioned medium, with or without verteporfin pretreatment. The expression of α-SMA

Figure 4. Characterization of primary HTFs. (A) Representative phase-contrast images of HTFs on days 3, 5 and 10. *Scale bar*: 100 μm. (B) Cells were stained with anti-vimentin antibodies and DAPI. *Scale bar*: 10 μm.

A

Supernatant treatment

Control | M2

0 h

22 h

B
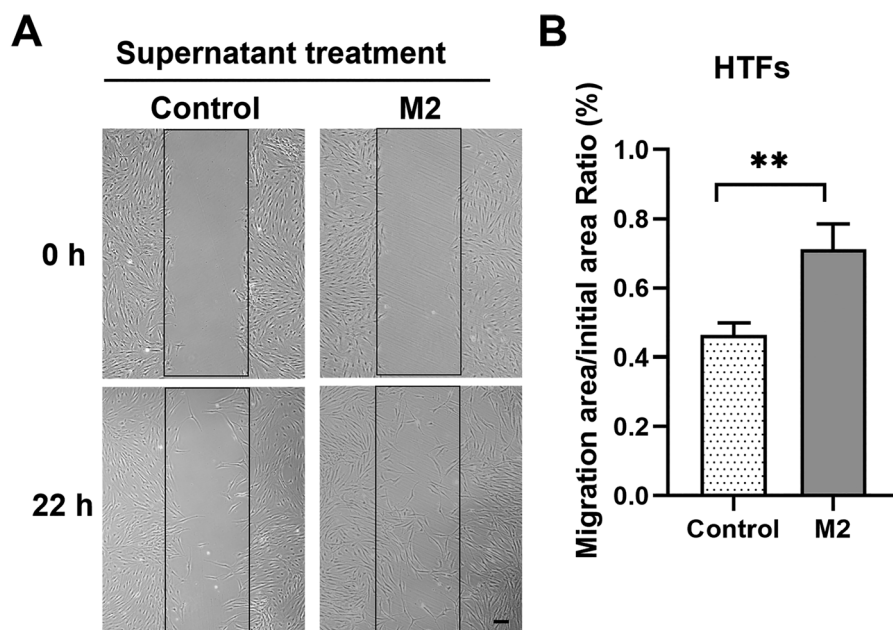
HTFs

Figure 5. M2 supernatant promoted the migration of primary HTFs in wound healing assay. HTFs were cultured with M2-conditioned medium (M2 group) or fresh culture medium (control group). (A) Light microscopic images of the scratch wound area taken at 0 and 22 h in the presence or absence of M2 supernatant. *Scale bar*: 100 μm. (B) Quantitative analysis of the ratio of the cellular migration area to the initial scratch area; the initial scratch area in each group was set as 100%. All experiments were repeated three times independently. **$P < 0.01$.

($P < 0.001$; Figure 6A,B), collagen I ($P < 0.01$; Figure 6C,D) and fibronectin ($P < 0.05$; Figure 6E,F) was significantly increased in HTFs cultured in M2-conditioned medium compared to that in the control. Verteporfin pretreatment effectively decreased the expression of α-SMA ($P < 0.01$; Figure 6A,B), collagen I ($P < 0.01$; Figure 6C,D) and fibronectin ($P < 0.05$; Figure 6E,F) stimulated by the M2-conditioned medium. These results indicate that YAP signalling may be involved in M2-induced myofibroblast activation in HTFs.

Mechanisms underlying the M2-induced fibrotic process in HTFs

Figure 7A,B shows the protein levels of collagen I, fibronectin and the components of TGF-β1/Smad2/3-YAP/TAZ signalling in the presence or absence of M2-conditioned medium. As expected, the M2-conditioned medium enhanced the protein expression of collagen I, fibronectin, TGF-β1, TGF-βR II and p-Smad2/3 ($P < 0.05$, *vs.* blank control). More interestingly, M2-conditioned medium induced higher expression of YAP and TAZ in HTFs than in the blank control ($P < 0.05$). These data further suggested an association between YAP/TAZ and the canonical TGF-β1 signalling pathway.

To verify the role of YAP/TAZ in M2-induced fibrosis, HTFs were pretreated with verteporfin. As shown in Figure 7A,B, verteporfin significantly reduced the

protein expression of collagen I and fibronectin. The expressions of YAP, TAZ and TEF1 were significantly downregulated by verteporfin treatment. Moreover, verteporfin decreased the expression of TGF-βR II and Smad2/3 and prevented the phosphorylation of Smad2/3.

Taken together, these data indicate that the interaction between YAP/TAZ and TGF-β1/Smad2/3 signalling may contribute to M2-induced myofibroblast activation in HTFs.

Discussion

Subconjunctival fibrosis remains a prominent challenge in surgical interventions for the treatment of glaucoma and other ocular surface conditions [30, 31]. M2 macrophages have been shown to promote wound repair and tissue fibrosis [2, 3, 5]. However, the roles of M2 macrophages in subconjunctival fibrosis remains underexplored. Herein, we found that dense collagen deposition around silicone was positively correlated with M2 infiltration in the early recovery phase after surgery. Our results showed that the M2 macrophage supernatant was rich in TGF-β1 and activated HTFs into myofibroblasts *in vitro*. Verteporfin inhibits myofibroblast activation. These findings indicate that crosstalk between YAP/TAZ and TGF-β1/Smad2/3 signalling may contribute to M2-induced HTF activation.
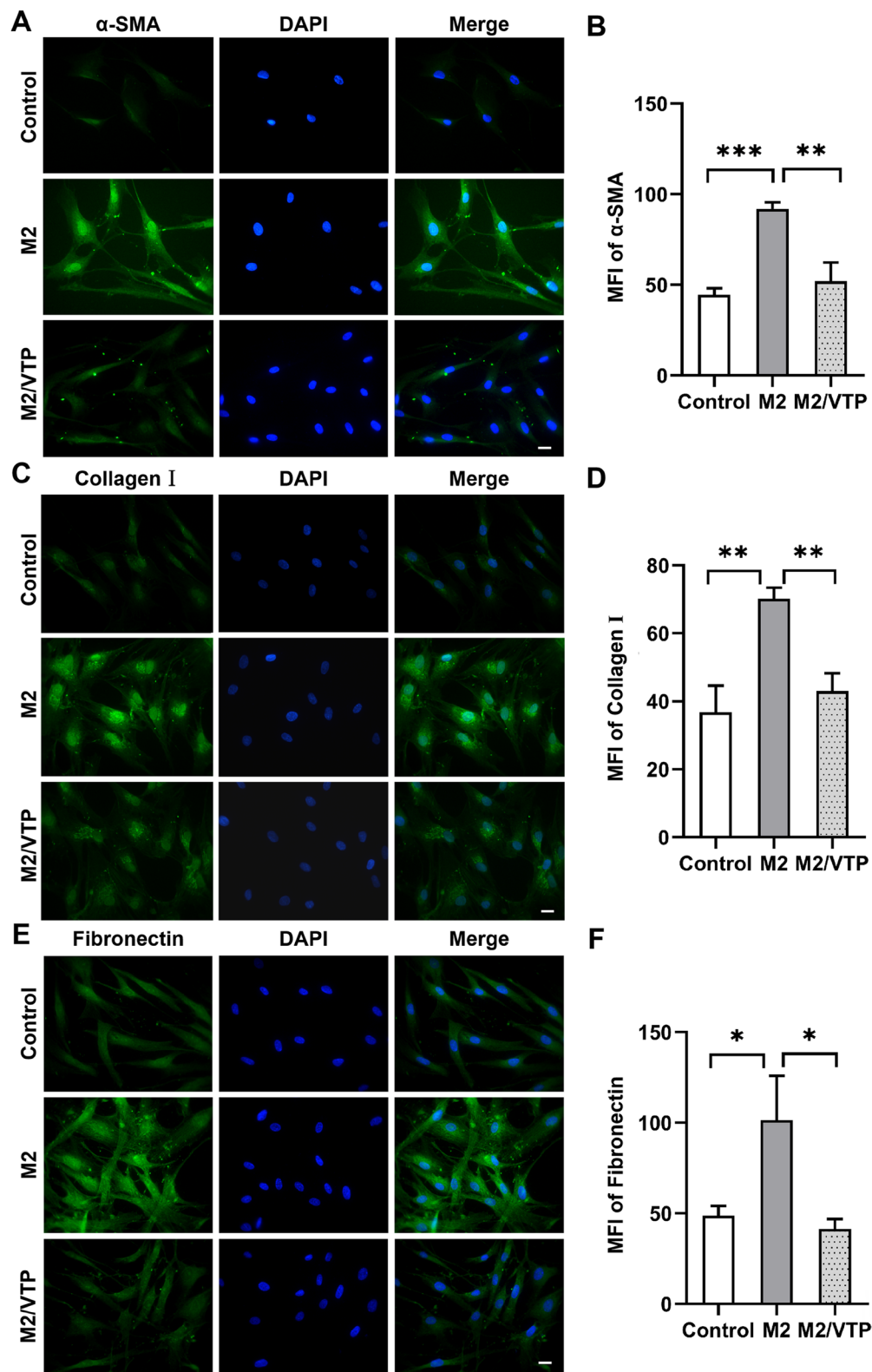
Figure 6. M2 supernatant promoted HTF activation and ECM synthesis. HTFs were treated with fresh culture medium (control), M2-conditioned medium only and verteporfin (VTP) (1.5 μmol/L, 3 h) followed by M2-conditioned medium treatment (M2/VTP) for 24 h. The expression levels of α-SMA, collagen I and fibronectin were evaluated by immunofluorescence staining. (A) Representative immunofluorescence images of HTFs stained with an anti-α-SMA antibody. *Scale bars*: 10 μm. (B) Quantitative analysis of the MFI of α-SMA. **$P < 0.01$, ***$P < 0.001$; $n = 3$. (C) Representative immunofluorescence images of HTFs stained with an anti-collagen I antibody. *Scale bars*: 10 μm. (D) Quantitative analysis of the MFI of collagen I. **$P < 0.01$; $n = 3$. (E) Representative immunofluorescence images of HTFs stained with an anti-fibronectin antibody. (F) Quantitative analysis of the MFI of fibronectin. *$P < 0.05$; $n = 3$. All experiments were repeated three times independently.
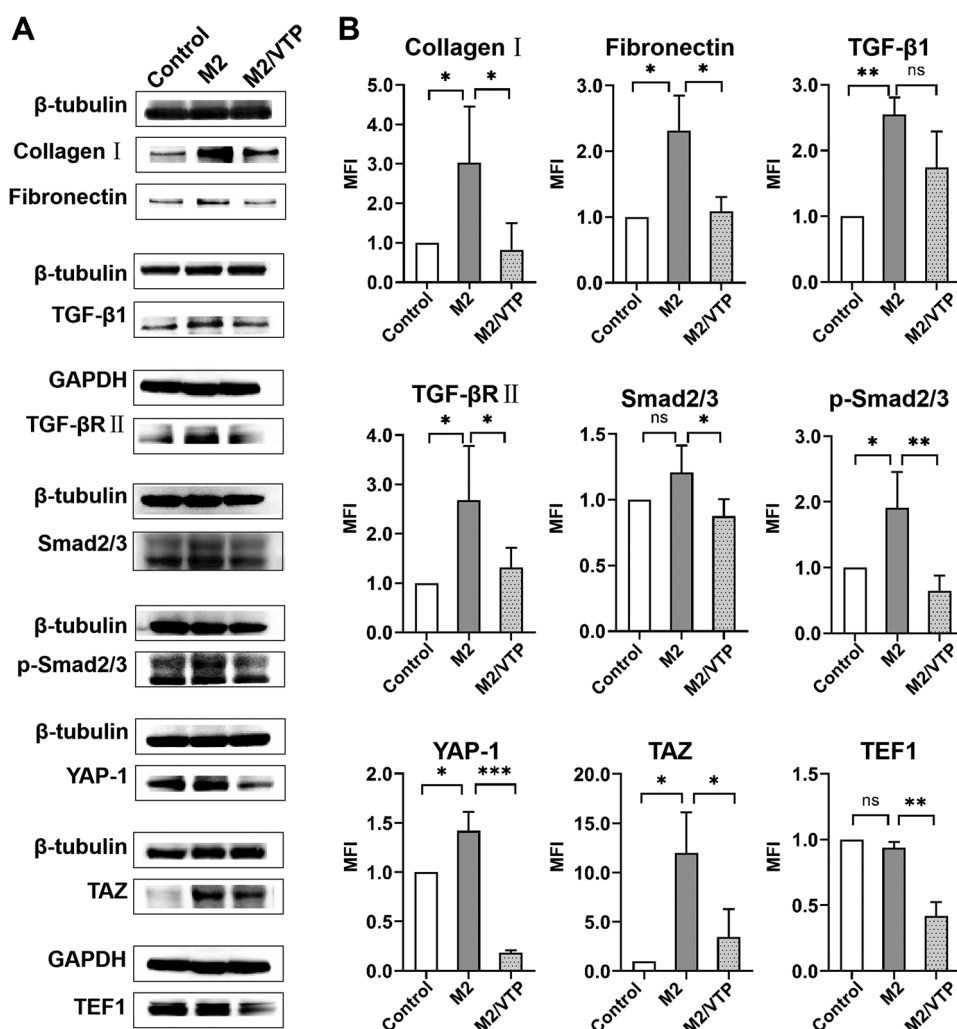
Figure 7. Crosstalk between YAP/TAZ and canonical TGFβ/Smad signalling contributed to M2 macrophage-induced fibrosis in HTFs. HTFs were treated with the fresh culture medium (control), M2-conditioned medium only and verteporfin (1.5 μmol/L, 3 h) followed by M2-conditioned medium treatment (M2/VTP) for 36 h. Protein levels of collagen I, fibronectin, YAP, TAZ and components of TGF-β1/smad signalling were determined by western blotting. (A) Representative images of western blot images. (B) Analysis of relative protein expression. GAPDH or β-tubulin was used as a loading control, as appropriate. *$P < 0.05$, **$P < 0.01$, ***$P < 0.001$; $n = 3$. All experiments were repeated three times independently. ns, not significant.

Macrophages exhibit high phenotypic and genetic plasticity. Depending on the microenvironment, macrophages can acquire distinct functional phenotypes (M1 *versus* M2 polarization) [4, 32]. M2 macrophages are typically considered 'pro-healing'. Although prior studies have reported the presence of macrophages in subconjunctival lesions and failed blebs [33–35], there is little information on the role of M2 macrophages in subconjunctival fibrosis. Prior study reported that macrophages existed on a continuum of polarization states between M1 and M2 following tissue injury [36]. The ratio of M1 and M2 phenotypes altered about 5–7 days after skin injury in mice [37]. Clinical specimens from patients with failed AGV surgery may only show pathological changes during the late remodelling period. Therefore, we established an animal model to mimic

early wound healing after AGV surgery. In the present study, we found a large amount of M2 macrophages in subconjunctival tissue surrounding silicone implant at 2 weeks after surgery. Our results indicate that the macrophage population shifted to an alternatively activated phenotype during the early recovery phase. Since the phenotypic polarization of macrophages is a dynamic process that responds to signals in the microenvironment [4, 20], this study did not reveal the entire picture of the phenotypes of macrophages in the subconjunctival tissue around glaucoma implant device. Further research is required in this regard. Nevertheless, our data can enrich the understanding of M2 macrophage activity in subconjunctival fibrosis.

Fibrotic encapsulation at surgery site is one major cause of AGV failure [35, 38]. Subconjunctival

perivalvular fibrosis may result from wound healing response and immune reaction to silicone implants, in which M2 macrophages are proposed to play an important role. We found thick collagen deposits surrounding the silicone fragments, which supported the conclusions of prior studies [35, 38]. Given that these silicone fragments had no filtering function, our model could not perfectly reflect the effect of aqueous humor on perivalvular fibrosis. However, to a certain extent, it can serve as a handy animal model for research on subconjunctival fibrosis.

Culturing human monocyte-derived macrophages is a useful tool for studying macrophages *in vitro*. We followed a classical protocol for M2 polarization, in which THP-1 cells were incubated with PMA and sequentially with IL4 and IL13 [39, 40]. The JAK/STAT signalling pathway is pivotal in macrophage polarization, and STAT6 is a crucial transcription factor in IL4- and IL13-mediated M2 polarization [39]. We identified significant phospho-STAT6 expression in THP-1-derived macrophages, which indicates M2 polarization. Moreover, IL4/IL13-treated cells showed a high expression of CD206. Furthermore, the expression of TGF-β1 increased after IL4/IL13 treatment, which is consistent with the notion that M2 macrophages are the main source of TGF-β1 [5]. Thus, the biological role of M2 may be related to the secretion of TGF-β1.

In vitro studies have shown that M2 macrophages promote fibrogenic activities in mouse lung epithelial cells [41], murine corneal fibroblasts [42] and human skin fibroblasts [13, 14]. However, the specific roles of M2 macrophages in HTF fibrosis are unclear. The TGF-β superfamily of proteins plays a critical role in tissue fibrosis. In contrast to TGF-β2, which has predominantly been detected in the aqueous humor [43, 44], TGF-β1 is ubiquitously expressed and its target receptors have been identified in most cell types. TGF-β1 binds to the serine and threonine kinase receptor TGF-βR II as a homodimer; TGF-βR II then recruits and activates TGF-βRII to activate intracellular signalling via the transcription factor Smad-2/3 [45,46]. Phosphorylated Smad2/3 accumulates in the nucleus and induces the transcription of profibrotic genes. There is ample evidence that TGF-β signalling via Smads plays a central role in the development of fibrosis in conjunctival wound healing [47]. Our study demonstrated that M2-conditioned medium significantly induced the synthesis of ECM in HTFs and promoted cell migration. Moreover, TGF-β1-induced Smad2/3 phosphorylation was observed in response to M2-conditioned medium. These findings suggest that canonical TGF-β1 signalling may be involved in the communication between M2 macrophages and HTFs.

ECM deposition increases stiffness of the microenvironment. YAP and TAZ are key mechanotransducers that can convey mechanical signals associated with ECM stiffness to many intracellular signals [48]. Notably, YAP/TAZ has been shown to interact with TGF-β signalling by regulating the cytoplasmic/nuclear shuttling of Smads [23–25, 49]. Consistent with these results, the expression levels of YAP and TAZ were increased in response to M2-conditioned medium treatment in our study. Moreover, Smad2/3 phosphorylation was observed, suggesting that TGF-β1/Smad2/3-YAP/TAZ signalling may be involved in M2-induced activation of HTFs.

To further test this hypothesis, we blocked YAP/TAZ signalling using verteporfin, a benzoporphyrin derivative that is clinically used for the ocular photodynamic treatment of neovascular macular degeneration [50]. This drug has been reported to have highly potent YAP inhibitory activity in the absence of light activation. Recently, Akiko Futakuchi and colleagues reported that YAP/TAZ was essential regulator of TGF-β2-mediated conjunctival fibrosis and verteporfin suppressed TGF-β2-fibrotic changes in conjunctival fibroblasts [24]. Similarly, we found that TGF-βR II and phosphorylated Smad2/3 protein levels were significantly decreased after verteporfin treatment, which was accompanied by decreased YAP/TAZ expression. Our study indicated that verteporfin suppressed the crosstalk between HTFs and M2 cells and attenuated M2-induced fibrotic activities. Taken together, our findings suggest that the crosstalk between YAP/TAZ and Smad2/3 may be at least partly involved in M2 macrophage-induced fibrosis.

The current study has two main limitations. Firstly, communications between macrophages and fibroblasts are very complicated. Our study focused on TGF-β1/Smad2/3-YAP/TAZ signalling, which did not reveal the full contents. Thus, we cannot conclude that M2 cells promoted fibroblasts only by TGF-β1/Smad2/3-YAP/TAZ pathway. There may be other mechanisms involved in cell-cell talk between M2 macrophages and fibroblasts. Further studies are needed. Secondly, we did not use inhibitors of YAP or deplete M2 macrophages in surgical wound to verify the roles of M2 cells in subconjunctival fibrosis *in vivo*. However, this study may be inspiring; macrophages or other upstream mediators of fibroblast activation may serve as targets for anti-fibrotic therapeutics.

In conclusion, the current study revealed a key role of M2 macrophages in subconjunctival fibrosis. TGF-β1/Smad2/3-YAP/TAZ signalling may contribute to M2-induced myofibroblast activation in HTFs. M2 macrophage may be a promising potential target for anti-fibrotic treatments in the future.

Authors contributions

Yiwei Wang: investigation, methodology, writing—original draft preparation and funding acquisition. Xingchen Geng: investigation, methodology, writing—original draft preparation. Zhihua Guo: investigation, methodology. Dandan Chu: investigation, methodology. Ruixing Liu: investigation, methodology. Boyuan Cheng: data curation and formal analysis. Haohao Cui: data curation and formal analysis. Chengcheng Li: data curation and formal analysis. Jingguo Li: conceptualization, funding acquisition, project administration, resources, supervision, validation, writing, review and editing. Zhanrong Li: conceptualization, funding acquisition, investigation, methodology, project administration, resources, supervision, validation, writing, review and editing.

Disclosure statement

Funding

ORCID

Jingguo Li http://orcid.org/0000-0002-0471-4540
Yiwei Wang http://orcid.org/0000-0002-8447-9631

Data availability statement

The data that support the findings of this study are available from the corresponding author, Z. Li, upon reasonable request.

References

[1] Wynn TA, Vannella KM. Macrophages in tissue repair, regeneration, and fibrosis. Immunity. 2016;44(3):1–15. doi: 10.1016/j.immuni.2016.02.015.

[2] Willenborg S, Eming SA. Cellular networks in wound healing. Science. 2018;362(6417):891–892. doi: 10.1126/science.aav5542.

[3] Smigiel KS, Parks WC. Macrophages, wound healing, and fibrosis: recent insights. Curr Rheumatol Rep. 2018;20(4):17. doi: 10.1126/science.aav5542.

[4] Murray PJ. Macrophage polarization. Annu Rev Physiol. 2017;79(1):541–566. doi: 10.1146/annurev-physiol-022516-034339.

[5] Gieseck RL3rd, Wilson MS, Wynn TA. Type 2 immunity in tissue repair and fibrosis. Nat Rev Immunol. 2018;18(1):62–76. doi: 10.1038/nri.2017.90.

[6] Murray PJ, Allen JE, Biswas SK, et al. Macrophage activation and polarization: nomenclature and experimental guidelines. Immunity. 2014;41(1):14–20. doi: 10.1016/j.immuni.2014.06.008.

[7] Wang Y, Zhang L, Wu GR, et al. MBD2 serves as a viable target against pulmonary fibrosis by inhibiting macrophage M2 program. Sci Adv. 2021;7(1):eabb6075. doi: 10.1126/sciadv.abb6075.

[8] Wang J, Xu L, Xiang Z, et al. Microcystin-LR ameliorates pulmonary fibrosis via modulating CD206(+) M2-like macrophage polarization. Cell Death Dis. 2020;11(2):136. doi: 10.1038/s41419-020-2329-z.

[9] Chen B, Yang Y, Yang C, et al. M2 macrophage accumulation contributes to pulmonary fibrosis, vascular dilatation, and hypoxemia in rat hepatopulmonary syndrome. J Cell Physiol. 2021;236(11):7682–7697. doi: 10.1002/jcp.30420.

[10] Yang G, Yang Y, Liu Y, et al. Regulation of alveolar macrophage death in pulmonary fibrosis: a review. Apoptosis. 2023;28(11–12):1505–1519. doi: 10.1007/s10495-023-01888-4.

[11] Kim MG, Kim SC, Ko YS, et al. The role of M2 macrophages in the progression of chronic kidney disease following acute kidney injury. PLoS One. 2015;10(12):e0143961. doi: 10.1371/journal.pone.0143961.

[12] Tang PM, Nikolic-Paterson DJ, Lan HY. Macrophages: versatile players in renal inflammation and fibrosis. Nat Rev Nephrol. 2019;15(3):144–158. doi: 10.1038/s41581-019-0110-2.

[13] Zhu Z, Ding J, Ma Z, et al. Alternatively activated macrophages derived from THP-1 cells promote the fibrogenic activities of human dermal fibroblasts. Wound Repair Regen. 2017;25(3):377–388. doi: 10.1111/wrr.12532.

[14] Gu S, Dai H, Zhao X, et al. AKT3 deficiency in M2 macrophages impairs cutaneous wound healing by disrupting tissue remodeling. Aging. 2020;12(8):6928–6946. doi: 10.18632/aging.103051.

[15] Peet C, Ivetic A, Bromage DI, et al. Cardiac monocytes and macrophages after myocardial infarction. Cardiovasc Res. 2020;116(6):1101–1112. doi: 10.1093/cvr/cvz336.

[16] Kim Y, Nurakhayev S, Nurkesh A, et al. Macrophage polarization in cardiac tissue repair following myocardial infarction. Int J Mol Sci. 2021;22(5):2715. doi: 10.3390/ijms22052715.

[17] Cao X, Shen D, Patel MM, et al. Macrophage polarization in the maculae of age-related macular degeneration: a pilot study. Pathol Int. 2011;61(9):528–535. doi: 10.1111/j.1440-1827.2011.02695.x.

[18] Zhou Y, Yoshida S, Nakao S, et al. M2 macrophages enhance pathological neovascularization in the mouse model of oxygen-induced retinopathy. Invest Ophthalmol Vis Sci. 2015;56(8):4767–4777. doi: 10.1167/iovs.14-16012.

[19] Xu N, Bo Q, Shao R, et al. Chitinase-3-like-1 promotes M2 macrophage differentiation and induces choroidal neovascularization in neovascular age-related macular degeneration. Invest Ophthalmol Vis Sci. 2019;60(14):4596–4605. doi: 10.1167/iovs.19-27493.

[20] Vannella KM, Wynn TA. Mechanisms of organ injury and repair by macrophages. Annu Rev Physiol. 2017;79(1):593–617. doi: 10.1146/annurev-physiol-022516-034356.

[21] Mia MM, Singh MK. New insights into Hippo/YAP signaling in fibrotic diseases. Cells. 2022;11(13):2065. doi: 10.3390/cells11132065.

[22] Meng Z, Moroishi T, Guan KL. Mechanisms of hippo pathway regulation. Genes Dev. 2016;30(1):1–17. doi: 10.1101/gad.274027.115.

[23] Futakuchi A, Inoue T, Wei FY, et al. YAP/TAZ are essential for TGF-β2-mediated conjunctival fibrosis. Invest Ophthalmol Vis Sci. 2018;59(7):3069–3078. doi: 10.1167/iovs.18-24258.

[24] Nakamura R, Hiwatashi N, Bing R, et al. Concurrent YAP/TAZ and SMAD signaling mediate vocal fold fibrosis. Sci Rep. 2021;11(1):13484. doi: 10.1038/s41598-021-92871-z.

[25] He X, Tolosa MF, Zhang T, et al. Myofibroblast YAP/TAZ activation is a key step in organ fibrogenesis. JCI Insight. 2022;7(4):e146243. doi: 10.1172/jci.insight.146243.

[26] Grannas K, Arngården L, Lönn P, et al. Crosstalk between hippo and TGFβ: subcellular localization of YAP/TAZ/smad complexes. J Mol Biol. 2015;427(21):3407–3415. doi: 10.1016/j.jmb.2015.04.015.

[27] Li Z, Liu R, Guo Z, et al. Celastrol-based nanomedicine promotes corneal allograft survival. J Nanobiotechnol. 2021;19(1):341. doi: 10.1186/s12951-021-01079-w.

[28] Tong J, Fu Y, Xu X, et al. TGF-β1 stimulates human Tenon's capsule fibroblast proliferation by miR-200b and its targeting of p27/kip1 and RND3. Invest Ophthalmol Vis Sci. 2014;55(4):2747–2756. doi: 10.1167/iovs.13-13422.

[29] Cai X, Yang Y, Chen P, et al. Tetramethylpyrazine attenuates transdifferentiation of TGF-β2-treated human Tenon's fibroblasts. Invest Ophthalmol Vis Sci. 2016;57(11):4740–4748. doi: 10.1167/iovs.16-19529.

[30] Schlunck G, Meyer-ter-Vehn T, Klink T, et al. Conjunctival fibrosis following filtering glaucoma surgery. Exp Eye Res. 2016;142:76–82. doi: 10.1016/j.exer.2015.03.021.

[31] Shu DY, Lovicu FJ. Myofibroblast transdifferentiation: the dark force in ocular wound healing and fibrosis. Prog Retin Eye Res. 2017;60:44–65. doi: 10.1016/j.preteyeres.2017.08.001.

[32] Das A, Sinha M, Datta S, et al. Monocyte and macrophage plasticity in tissue repair and regeneration. Am J Pathol. 2015;185(10):2596–2606. doi: 10.1016/j.ajpath.2015.06.001.

[33] Sheridan CM, Unger WG, Ayliffe W, et al. Macrophages during fibrosis following scleral fistulising surgery in a rat model. Curr Eye Res. 1996;15(5):559–568. doi: 10.3109/02713689609000767.

[34] Shima I, Katsuda S, Ueda Y, et al. Expression of matrix metalloproteinases in wound healing after glaucoma filtration surgery in rabbits. Ophthalmic Res. 2007;39(6):315–324. doi: 10.1159/000109987.

[35] Thieme H, Choritz L, Hofmann-Rummelt C, et al. Histopathologic findings in early encapsulated blebs of young patients treated with the Ahmed glaucoma valve. J Glaucoma. 2011;20(4):246–251. doi: 10.1097/IJG.0b013e3181e080ef.

[36] Martin KE, García AJ. Macrophage phenotypes in tissue repair and the foreign body response: implications for biomaterial-based regenerative medicine strategies. Acta Biomater. 2021;133:4–16. doi: 10.1016/j.actbio.2021.03.038.

[37] Hesketh M, Sahin KB, West ZE, et al. Macrophage phenotypes regulate scar formation and chronic wound healing. Int J Mol Sci. 2017;18(7):1545. doi: 10.3390/ijms18071545.

[38] Fatehi N, Morales E, Parivisutt N, et al. Long-term outcome of second Ahmed valves in adult glaucoma. Am J Ophthalmol. 2018;186:96–103. doi: 10.1016/j.ajo.2017.11.018.

[39] Genin M, Clement F, Fattaccioli A, et al. M1 and M2 macrophages derived from THP-1 cells differentially modulate the response of cancer cells to etoposide. BMC Cancer. 2015;15(1):577. doi: 10.1186/s12885-015-1546-9.

[40] Li X, Leng Y, Jiang Q, et al. Eye drops of metformin prevents fibrosis after glaucoma filtration surgery in rats via activating AMPK/Nrf2 signaling pathway. Front Pharmacol. 2020;11:1038. doi: 10.3389/fphar.2020.01038.

[41] Zhu L, Fu X, Chen X, et al. M2 macrophages induce EMT through the TGF-β/Smad2 signaling pathway. Cell Biol Int. 2017;41(9):960–968. doi: 10.1002/cbin.10788.

[42] Corpuz AB. Role of macrophages in ocular surface fibrosis [master's thesis]. Irvine (CA): Chapman University; 2022. doi: 10.36837/chapman.000407.

[43] Tripathi RC, Li J, Chan WF, et al. Aqueous humor in glaucomatous eyes contains an increased level of TGF-beta 2. Exp Eye Res. 1994;59(6):723–727. doi: 10.1006/exer.1994.1158.

[44] Inatani M, Tanihara H, Katsuta H, et al. Transforming growth factor-beta 2 levels in aqueous humor of glaucomatous eyes. Graefes Arch Clin Exp Ophthalmol. 2001;239(2):109–113. doi: 10.1007/s004170000241.

[45] Meng XM, Nikolic-Paterson DJ, Lan HY. TGF-β: the master regulator of fibrosis. Nat Rev Nephrol. 2016;12(6):325–338. doi: 10.1038/nrneph.2016.48.

[46] Frangogiannis N. Transforming growth factor-β in tissue fibrosis. J Exp Med. 2020;217(3):e20190103. doi: 10.1084/jem.20190103.

[47] Zada M, Pattamatta U, White A. Modulation of fibroblasts in conjunctival wound healing. Ophthalmology. 2018;125(2):179–192. doi: 10.1016/j.ophtha.2017.08.028.

[48] Nukuda A, Sasaki C, Ishihara S, et al. Stiff substrates increase YAP-signaling-mediated matrix metalloproteinase-7 expression. Oncogenesis. 2015;4(9):e165–e165. doi: 10.1038/oncsis.2015.24.

[49] Szeto SG, Narimatsu M, Lu M, et al. YAP/TAZ are mechanoregulators of TGF-β-Smad signaling and renal fibrogenesis. J Am Soc Nephrol. 2016;27(10):3117–3128. doi: 10.1681/ASN.2015050499.

[50] Brown SB, Mellish KJ. Verteporfin: a milestone in opthalmology and photodynamic therapy. Expert Opin Pharmacother. 2001;2(2):351–361. doi: 10.1517/14656566.2.2.351.